Chemical Engineering Journal 326 (2017) 640–646

Contents lists available at ScienceDirect

Chemical Engineering Journal

journal homepage: www.elsevier.com/locate/cej

Highly efficient oil/water separation and trace organic contaminants removal based on superhydrophobic conjugated microporous polymer coated devices

Zhenyu Xiao, Minghui Zhang, Weidong Fan, Yunyang Qian, Zhendong Yang, Ben Xu, Zixi Kang, Rongming Wang, Daofeng Sun *

State Key Laboratory of Heavy Oil Processing, College of Science, China University of Petroleum (East China), Qingdao, Shandong 266580, PR China

HIGHLIGHTS

- Two kinds of conjugated microporous polymers coated superhydrophobic devices were first reported.
- The polymer coated stainless steel mesh shows highly oil/water separation efficiency.
- Large-scale removing of organic pollution can be realized by polymer-coated sponge.
- The trace residual and solved aromatic pollutions can be removed by polymer-coated sponge.

GRAPHICAL ABSTRACT

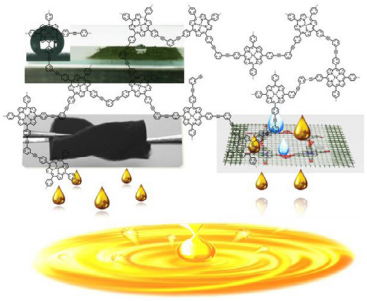

ARTICLE INFO

Article history:
Received 5 March 2017
Received in revised form 5 June 2017
Accepted 5 June 2017
Available online 10 July 2017

Keywords:
Superhydrophobicity
Conjugated microporous polymers
Oil/water separation
Water purification

ABSTRACT

Superhydrophobic iron(III) porphyrin-based conjugated microporous polymers (**CMPs**) are successfully coated on both stainless steel mesh and sponge framework, which are well utilized in separating oil and trace organic contaminants from water for the first time. Due to the superhydrophobic character of the material, the **CMP**-coated stainless steel and sponge both exhibit high oil/water separation efficiency through filtration and adsorption process, respectively. Furthermore, coated sponges can remove not only the large-scale organic solvents but also the trace organic contaminants from water, which make it an excellent candidate for applications of oil/water separation and water purification.

1. Introduction

Oil spill accidents, fuel used in marine transport and natural oil seeps have caused serious environmental pollution [1–4]. Over $10 billion dollars for the oil spill cleanup are consumed each year. Therefore, the efficient separation of oil from water would not only prevent the environmental pollution but also significantly reduce the economic losses by reusing the spilled oil [5,6]. Several oil-spill cleaning technologies were developed in the last decades, including floatation, filtration, centrifugation, separation, and electrochemical methods, in which the separation method holds great advantage due to its simplicity, low cost, and high efficiency [7–10]. However, this method requires specific materials which can effectively separate oil from water, and thus the preparation of these materials are in urgent demand and it is a challenging task.

As is known, the wettability of material surface is crucial for oil/water separation, which is highly dependent on the chemical composition and the geometrical microstructure [11–13]. As a result, in the past decade, plenty of efforts have been devoted to developing

* Corresponding author.
E-mail address: dfsun@upc.edu.cn (D. Sun).

http://dx.doi.org/10.1016/j.cej.2017.06.023
1385-8947/

surfaces with both hydrophobicity and oleophilicity through modifying chemical compositions or tuning geometrical microstructures of the materials for oil/water separation [8,14–16]. Based on past research, the materials can be used in two ways: the hydrophobic materials are directly used as the oil adsorbent for oil/water separation, or the hydrophobic materials are coated/applied on/to the meshes/fibres/textiles/sponge for direct separation [17–20]. It has been found that the latter method is more promising due to the relatively less material consumption in comparison with the former one. A lot of outstanding research has been done on coating meshes/fibres/textiles/sponge with low surface energy substances such as silicone nanofilaments, carbon nanotubes, and fluorochemicals. However, the working capacity and reusability of these materials remain the biggest problem when using in practice and it needs further improvement [3,21]. Consequently, new hydrophobic materials are highly desired in order to solve the aforementioned issues for practical applications.

Conjugated microporous polymers (**CMPs**) and/or covalent-organic frameworks (**COFs**) are a new class of porous materials that can be easily synthesized by common organic reactions such as Suzuki coupling, Sonogashira coupling, and condensation reaction [22–29]. Because of the easily adjusted surface nature, good stability, and large surface area, **CMPs** and/or **COFs** have received much research interests, and their physicochemical properties such as gas storage and catalysis have been widely studied. Yaghi and his coworkers pioneered the synthesis and applications of **COFs** based on various organic reactions [30–33]. Jiang group also synthesized a series of **CMPs** based on the metalloporphyrin building unit and studied their gas adsorption and heterogeneous catalysis properties [34–37]. However, studies on surface wettability of **CMPs** and/or **COFs** and their applications on oil/water separation have seldom been explored. Recently, Li and coworkers reported two superhydrophobic **CMPs** based on homocoupling polymerization of 1,3,5-triethynylbenzene. After loading the superhydrophobic **CMPs** on a sponge, it can efficiently adsorb octane and nitrobenzene [38]. However, rapid and efficient oil/water separation and water purification by superhydrophobic **CMP** coated devices have never been reported to date.

In this work, we report a superhydrophobic **CMP** material (**UPC-CMP-2**) based on iron(III) porphyrin unit. **UPC-CMP-2** could be coated on a stainless steel (SS) mesh for rapid and highly efficient oil/water separation. More importantly, **UPC-CMP-2** and analogues could be also easily coated on the framework of sponge to remove large-scale organic solvents, and adsorb trace or even dissolved organic contaminants. This work may provide a way for assembling various **CMP**-functionalized devices.

2. Results and discussion

2.1. Preparation and wettability of UPC-CMP-2

UPC-CMP-2 was synthesized by the Sonogashira-Hagihara coupling reaction of iron(III)-5,10,15,20-tetrakis-(4-bromophenyl)porphyrin and 1,3-diethynylbenzene. The original product was washed with water, methanol (MeOH), tetrahydrofuran (THF), and dichloromethane (CH_2Cl_2), and further purified by soxhlet extraction for four days using H_2O, MeOH, THF and CH_2Cl_2 as solvents to produce **UPC-CMP-2**. The geometry optimization result shows that **UPC-CMP-2** possesses a lattice-like structure, in which the benzene rings of 1,3-diethynylbenzene is seen as the linkers, and the coordinated chloride ions locate on the central iron(III) ions (Fig. 1a). The morphology of **UPC-CMP-2** was investigated by the scanning electron microscopy (SEM). As shown in Fig. 1g and h, **UPC-CMP-2** is of agglomerated dendrite-like nanostructure with diameter between 50 and 80 nm for the branch. Thermogravimetric analysis (TGA) shows that **UPC-CMP-2** possesses good thermal stability, which is stable up to 350 °C (Fig. S1). The FT-IR spectrum of **UPC-CMP-2** show weak alkyne's characteristic bands at 2208 cm^{-1}, which indicate 1,3-diethynylbenzene was successful involved in the network (Fig. S2). Due to the existence of Fe^{3+} ions with paramagnetic effect, the solid-state $^{1}H–^{13}C$ CP/MS of **UPC-CMP-2** was characterization by Fe-free porphyrin polymer (**P-CMP**). As shown in Fig. 1b and e, four remarkable broad peaks emerge at 154, 140, 132, and 119 ppm, which are assigned to the phenylene moiety and porphyrin macrocycle, respectively. The weak resonance peak at 86 ppm is attributed to the acetylene group. The permanent porosity of **UPC-CMP-2** was further checked by BET test and gas-uptake measurements (Figs. 1c and S15). As shown in Fig. 1c, **UPC-CMP-2** displays a typical Type-(I + IV) sorption isotherm with the BET surface area of 465.7 $m^2\ g^{-1}$ and pore widths centering at 1.5 and 2.8 nm (calculated by the nonlocalized density functional theory method, Fig. 1d), which is similar to our reported work (**UPC-CMP-1**) [39] and other **Fe-P-CMP** materials [40].

The surface wettability was investigated by performing the water contact angle measurement on the powder sample. **UPC-CMP-2** exhibits a water contact angle of 158°, indicating its superhydrophobic character. Additional experiments were also carried out by dropping water or diluted crude oil with hexane onto the surface of **UPC-CMP-2**. As shown in Fig. 2a, when water was dropped onto the surface of **UPC-CMP-2** by a syringe, the water droplet was formed with a big contact angle. In contrast, the diluted crude oil was rapidly spread on **UPC-CMP-2** (Fig. 2b), suggesting its oleophilicity. Moreover, **UPC-CMP-2** powders can float on water, but sink to the bottom in ethyl acetate (Fig. 2g), further indicating the superhydrophobic and oleophilic character. The superhydrophobicity should be attributed to the multi-ring aromatic hydrocarbons of **UPC-CMP-2**.

2.2. UPC-CMP-2 coated stainless steel mesh for oil/water separation

Due to both superhydrophobicity and oleophilicity, **UPC-CMP-2** can float on the water, but sinks into organic solvents (Fig. 2g). Hence, it is an ideal candidate for the application in oil/water separation. In order to reduce the consumption of **UPC-CMP-2** material, **UPC-CMP-2** was coated on the stainless steel mesh for the practical application of oil/water separation. The mesh used in this work was knitted into square pores using stainless steel wires with a diameter of about 0.7 mm. Scanning electron microscopy (SEM) images of uncoated mesh and coated mesh are shown in Figs. 2h–j and S4. The surfaces of the uncoated mesh are smooth and clear, but in contrast, the coated mesh has rough surfaces with numerous nanostructured branches on them, suggesting the successful coating of **UPC-CMP-2**. As expected, water could not pass through the coated mesh, and water droplet was formed with the contact angle of 152° (Fig. 2c, d), indicating that the coated mesh possesses a completely different surface wettability compared with the uncoated one. Accordingly, the coated mesh can float on the water while the uncoated one sinks (Fig. 2e, f). On the contrary, oil can easily pass through the coated mesh due to the oleophilicity of **UPC-CMP-2**. The aforementioned characters of the coated mesh together with its large openings make it very promising for rapid and efficient oil/water separation.

A series of practical oil/water separation experiments were performed by using a simple experimental setup, as shown in Fig. 3. The coated mesh was fixed between two plastic pipes to set up a simple filtration installation, and the pipes were placed with a tilt angle of 15° to ensure the contact of the tested organic solvents, including toluene ($PhCH_3$), hexane, petroleum ether (PE), gasoline, naphtha (NHT), diesel, and crude oil. In order to observe the effect clearly, water was dyed by acid red 18 to show vivid color. The

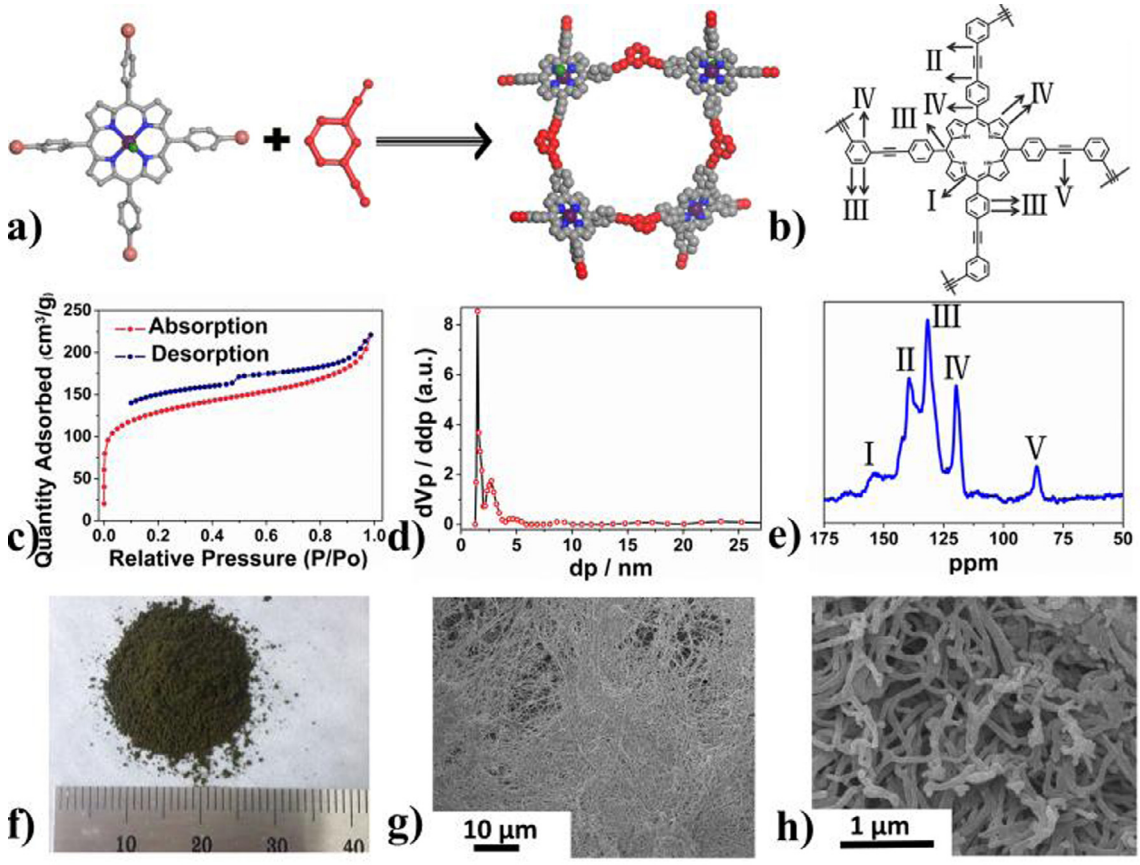

Fig. 1. (a) Synthetic route toward UPC-CMP-2. (b and e) The chemical shifts and solid-state ^{13}C NMR spectrum of Fe-free UPC-CMP-2. (c and d) N_2 sorption isotherm and pore size distribution of UPC-CMP-2. (f) Photographs of synthesized UPC-CMP-2. (g and h) SEM images of the as-synthesized UPC-CMP-2 with different magnifications.

tested objects and water solution were mixed in a syringe, and then injected into the pipe to ensure the sufficient contact of the mixtures with the coated mesh. When the mixture of water and hexane was injected into the pipe, water first contacted with the coated mesh but did not pass through it, but hexane passed through the coated mesh quickly and fell into the beaker beneath it to achieve relatively complete separation (Video 1 in the Supporting information). Similar the process, methylbenzene/water, petroleum ether/water, gasoline/water, naphtha/water, crude oil/water and diesel oil/water were also separated successfully. After the separation, there were no visible tested objects in water (Videos 2–7 in the Supporting information), indicating the separation was highly efficient.

To further evaluate the performance of the coated mesh on the oil/water separation, the separation efficiency was calculated using the oil rejection coefficient (R(%)) according to

$$R(\%) = \left(1 - \frac{C_s}{C_0}\right) \times 100$$

where C_0 and C_s are the oil content of the original oil/water mixtures and the collected water after the separation, respectively. Based on the calculation, the separation efficiency is in excess of 99.0% for all the tested objects, as shown in Fig. 4a. It is well known that diesel and crude oil are difficult to be separated efficiently from water owing to their complex composition and high viscosity, but the coated mesh keeps high-efficient diesel/water and crude oil/water separation properties with the separation efficiency being 99.3% and 99.8%, respectively. Since the reusability is another important factor that evaluates the performance of devices in practical applications, the process of hexane/water separation was repeated ten times. The results displayed that the separation efficiency was maintained (Fig. 4b), and the coated mesh can also keep a water contact angles of 156° after ten cycles (Fig. S3). To the best of our knowledge, this is the first example that the **CMP** material coated stainless steel mesh device is applied to rapid and efficient oil/water separation and water purification, and exhibits excellent separation efficiency and reusability.

2.3. Coating CMP on the sponge framework for Oil/Water separation and rapid removal of organic pollutants from water

On the basis of above investigations, we attempted to coat **UPC-CMP-2** on a sponge framework to realize the oil/water separation through a simple operation and lower energy consumption process. As shown in Fig. 5a–d, the smooth sponge framework was coated by laminated **UPC-CMP-2** with a thickness of about 200 nm, which makes the sponges hydrophobic and oleophilic. The coating mass of **UPC-CMP-2** is about 7.3 mg for each sponge with the size of $1.5 \times 1.5 \times 1.5\ cm^3$. As shown in Fig. 5e, when the blank and coated sponges were simultaneously placed in a water bath, the blank sponge absorbed water and sank into the bottom of beaker while the **UPC-CMP-2** coated one was floating on water. If **UPC-CMP-2** coated sponge was pressed in water, a layer of gas film on its surface can be clearly observed (Fig. 5f). As expected, the **UPC-CMP-2** coated sponge shows excellent oil/water separation and water purification ability. As shown in Fig. 5i, when a piece of **UPC-CMP-2** coated sponge was placed on the surface of ethyl acetate (EA) (dyed with red oil o) and water mixture, the sponge can almost completely absorb the floating ethyl acetate in 3 min. After taking out the sponge, the absorbed

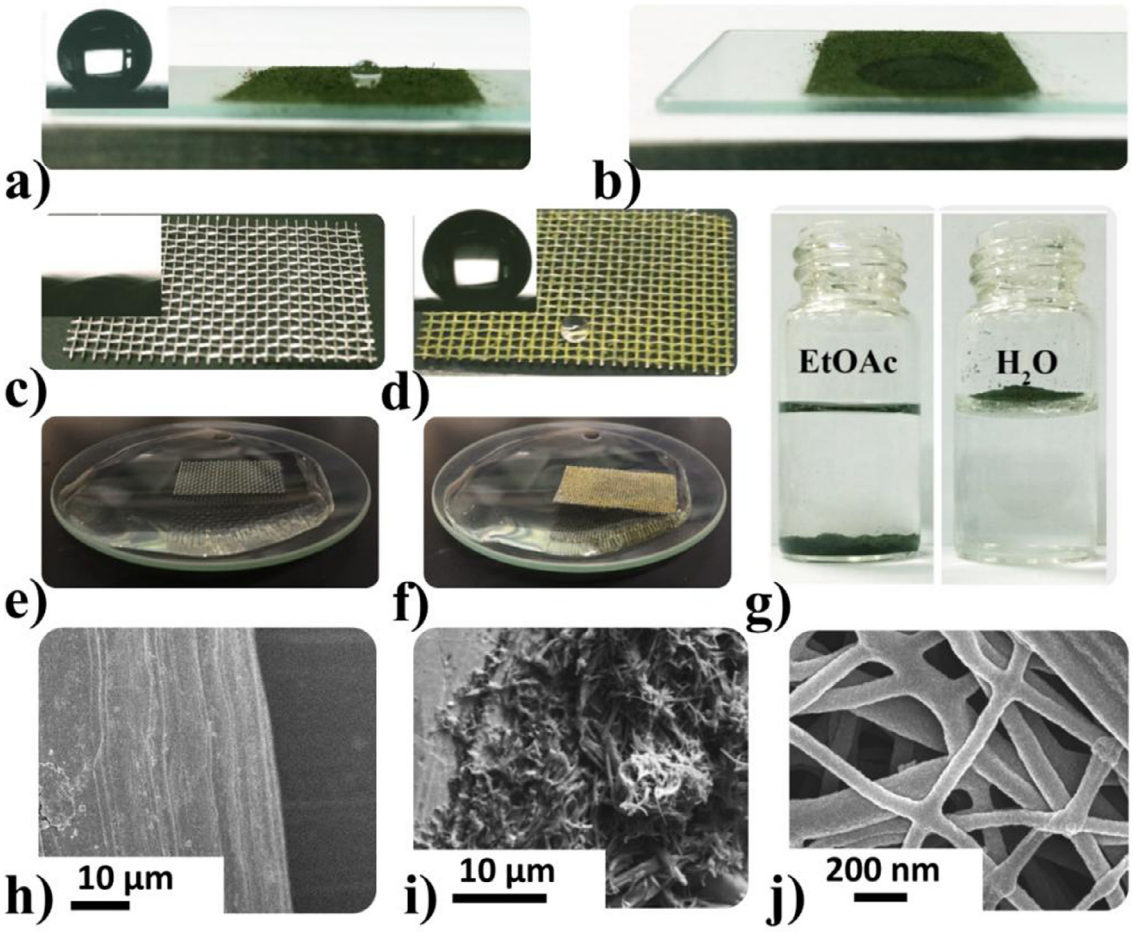

Fig. 2. (a) Photographs of UPC-CMP-2 with a water contact angle of 158°, and (b) an oil contact angle of 0°. (c and d) Photographs of water droplet on the stainless steel mesh without and with UPC-CMP-2 coating, respectively. Insert: the measurements of water contact angle. (e and f) The stainless steel meshes without and with UPC-CMP-2 coating sink and float in water, respectively. (g) UPC-CMP-2 can sink in ethyl acetate (left) and float on the water (right). (h) SEM image of the original stainless steel mesh. (i and j) SEM images of UPC-CMP-2 coated stainless steel mesh.

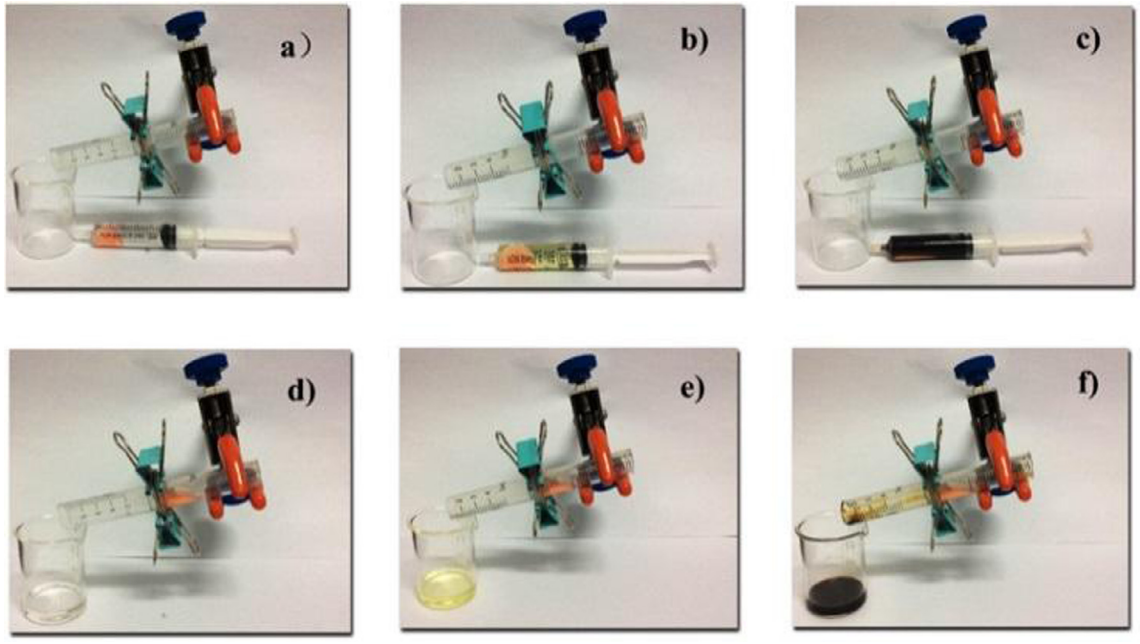

Fig. 3. Photographs of oil/water separation experiments. The initial and final states of separation experiments: toluene/water (a, d), gasoline/water (b, e), and crude oil/water (c, f).

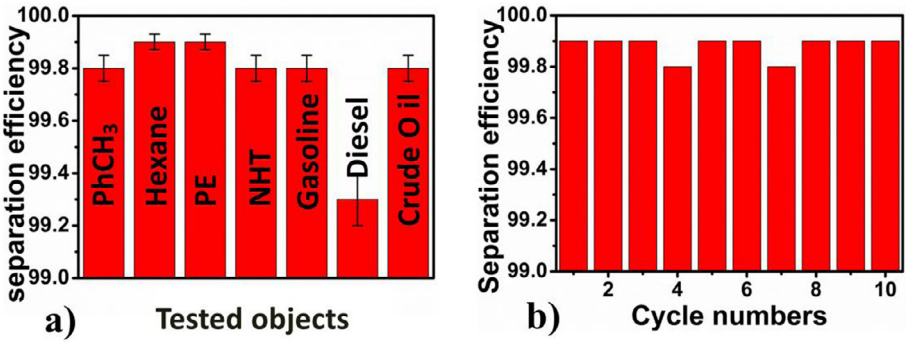

Fig. 4. Oil/water separation efficiency (a), and hexane/water separation cycle performance (b) of UPC-CMP-2 coated stainless steel mesh.

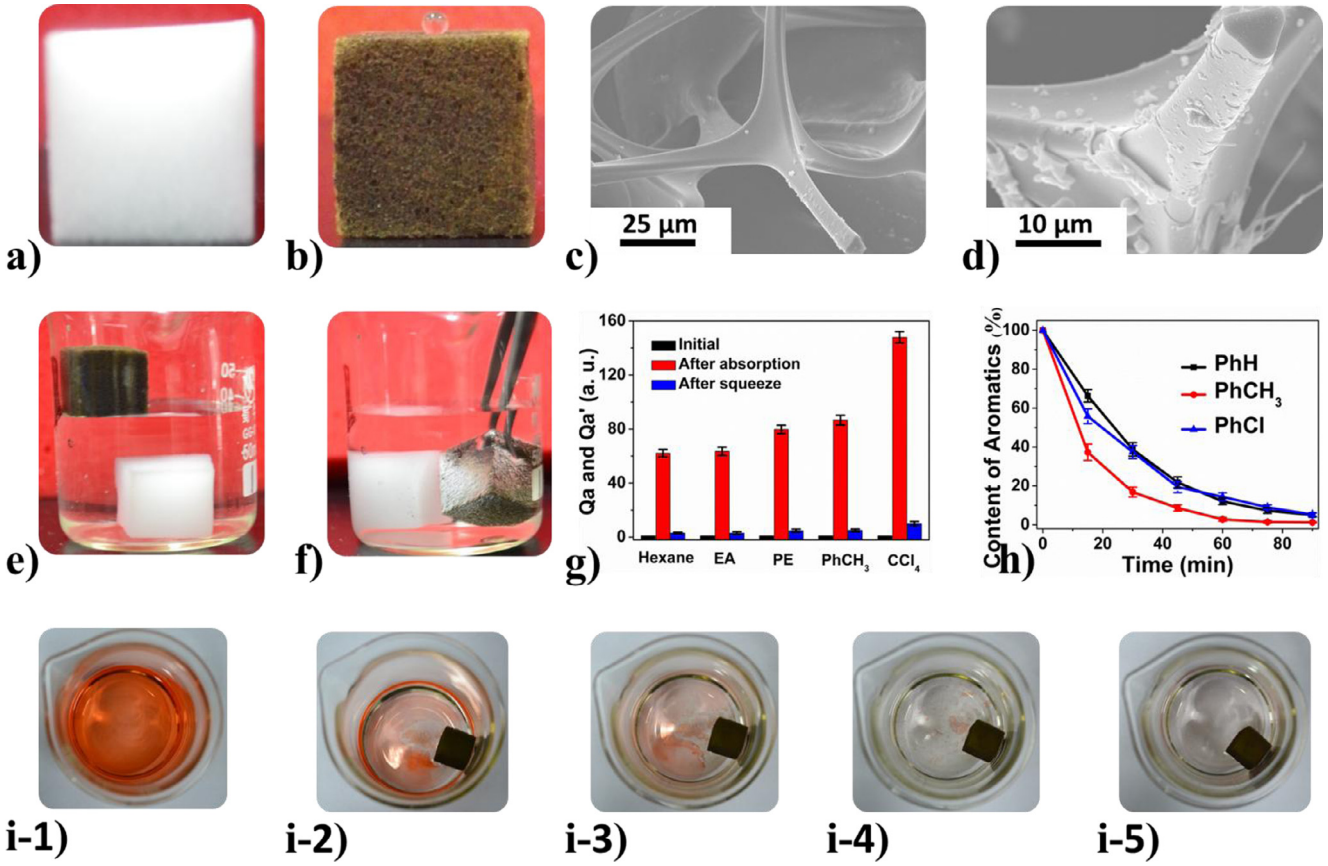

Fig. 5. (a and b) Photographs of water droplet on the sponge without and with coated UPC-CMP-2, respectively. (c and d) The SEM images of sponge before and after coating UPC-CMP-2. (e) The pristine sponge sinks into water, and the UPC-CMP-2 coated sponge floats on water. (f) The UPC-CMP-2 coated sponge was pressed below the water surface. (g) The Q_a and Q'_a of the UPC-CMP-2 coated sponges. (h) The adsorption curves of water solutions with different organic solvents in the presence of UPC-CMP-2 coated sponge. i 1–5) Snapshots showing ethyl acetate film (dyed by red oil o) were absorbed in UPC-CMP-2 coated sponge (1.5 × 1.5 × 1.5 cm).

ethyl acetate can be easily extracted through simple mechanical squeeze or distillation, and the sponge can be recycled and reused. In this experiment, the weight of blank coated sponge is 38.2 mg, but the total weight changes to 3295 mg after adsorbing ethyl acetate. The value means that the saturated absorptivity (defined as Q_a, the ratio between the final weight of coated sponge after the saturated absorption and the initial weight of coated sponge) of the coated sponge is nearly to 86.6 for ethyl acetate. After simple squeeze by hands, the residual weight of the coated sponge is about 207 mg, i.e., 3088 mg ethyl acetate can be recycled from oil/water mixture, which equals 80.8 times of own weight of coated sponge. As reported previously [36], **CMPs** often show excellent chemical stability and are totally insoluble in all organic solvents. Based on this unique physicochemical property, it would be natural to assume that **CMPs** can be used as absorbents for any kinds of organic solvents. Therefore, the similar adsorption experiments were conducted and repeated 6 times by using the above-mentioned size of coated sponge for different oil/water systems including water/hexane, water/petroleum ether (PE), water/-toluene ($PhCH_3$), water/ethyl acetate (EA) and water/carbon tetrachloride (CCl_4), as shown in Fig. 5g, and the average absorptivities are 60.7, 62.8, 79.8, 87.0 and 145.0 times of own weight, respectively. Because the **UPC-CMP-2** was coated on the framework of sponge with a very thin layer, the physical absorption of organic molecules in the sponge pores may be the mainly stored mechanism. Therefore, the Q_a values mainly depend on the density of

organic solvents. When the organic solvent has higher density, the Q_a is bigger such as CCl_4. Compared with the reported **HCMP-1** loaded sponges by Deng's group [38], the Q_a values are about 2 times higher than their results. These results show that the **UPC-CMP-2** coated sponge is an excellent candidate to realize large-scale removal or recycle of floating organic solvents.

In the practical oil/water separation process, the separated water is often inedible and poisonous as trace organic contaminants have been dispersed or dissolved in water. In this work, the water remains a pungent smell after the floating benzene is quickly removed by the **UPC-CMP-2** coated sponge, as the trace benzene dissolves in water. However, the pungent smell of benzene is almost disappeared after the **UPC-CMP-2** coated sponge was left in the mixture for 12 h. To further investigate the capability of the coated sponge to remove trace benzene, 2 ml benzene (PhH) was added to 80 ml water and ultrasonic for 24 h, and then a supersaturated benzene solution was sucked from the bottom of standing solution. After putting the recycled coated sponge into 60 ml saturated solution for 90 min, 95.0% of dissolved benzene was absorbed (Fig. S6). Similar procedures were conducted for toluene ($PhCH_3$) and chlorobenzene (PhCl), which are the common water pollutants and strong toxic carcinogens. The results showed that 98.7% of toluene and 94.8% of chlorobenzene were removed, respectively (Figs. 5h and S7, S8).

To further explore the effect of **UPC-CMP** coated sponge device on water purification, **UPC-CMP-1** and **UPC-CMP-3** coated sponges were prepared by replacing 1,3-diethynylbenzene with 1,4-diethynylbenzene and 1,3,5-triethynylbenzene in the synthesis process, respectively. The average coating mass of **UPC-CMP-1** in each sponge ($1.5 \times 1.5 \times 1.5\ cm^3$) is 6.4 mg, which is close to the coating weight of **UPC-CMP-2**, and the microstructure of coated **UPC-CMP-1** (Fig. 6a) is similar to **UPC-CMP-2**. However, the average coating mass of **UPC-CMP-3** is only 3.45 mg as the coated thickness is thinner than the one of **UPC-CMP-2** (Fig. 6b). The differences should be attributed to the molecular structure of 1,3,5-triethynylbenzene as it possesses a triangle connection geometry, which is different from linear bridging geometry of 1,3-diethynylbenzene and 1,4-diethynylbenzene. Meanwhile, **UPC-CMP-1** and **UPC-CMP-2** possess similar dendrite-like nanostructure (Figs. S5a and 1h), but **UPC-CMP-3** has globular-like nanostructure with the diameter between 500 nm and 600 nm (Fig. S5b). The water purification results of these sponges demonstrate that 94.18% and 92.6% of dissolved benzene, 99.7% and 81.1% of dissolved toluene, 87.4% and 87.3% of dissolved chlorobenzene can be absorbed by the **UPC-CMP-1** and **UPC-CMP-3** coated sponge in 90 min (Figs. 6c, d and S9–S14), respectively, which are slightly lower than those values of **UPC-CMP-2** coated sponge. We believe that the solved organic pollutions were mainly absorbed in the microporous of **CMP**, and the adsorption driving force could be mainly attributed to π-π interactions between organic contaminants and the large π-conjugated skeletons of **CMPs** [41]. So, the loading mass of **CMP** materials may be the prime reasons of these slight differences. The results indicate that **UPC-CMP-1**, **2**, **3** coated sponges will not only can remove large-scale oils, but also may absorb trace residual of organic contaminants, which may provide a potential method to solve the issues of oil pollutants and noxious trace residual.

3. Conclusions

In conclusion, by using a Sonogashira-Hagihara coupling reaction, a porous conjugated microporous polymer (**UPC-CMP-2**) has been synthesized based on iron (III) porphyrin building units. A series of characterizations indicate that **UPC-CMP-2** is a superhydrophobic material with the water contact angle of 158°. Interestingly, **UPC-CMP-2** can be easily coated on the surfaces of stainless steel mesh, and the coated mesh shows rapid and highly efficient oil/water separation efficiency. Meanwhile, the **UPC-CMP-2** and analogues (**UPC-CMP-1** and **UPC-CMP-3**) can also be easily coated

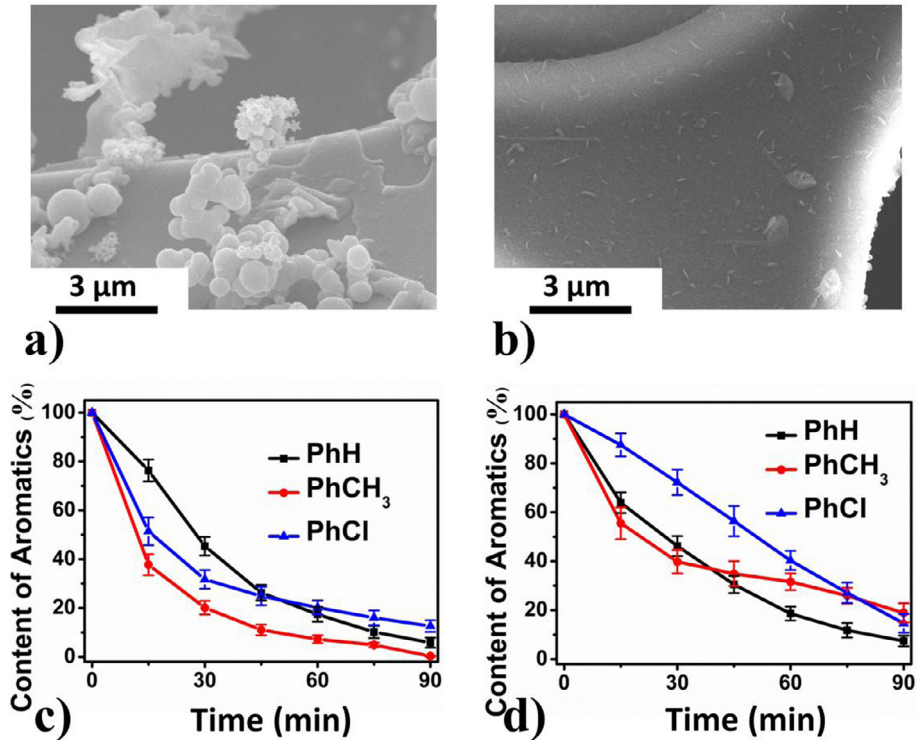

Fig. 6. The SEM images of UPC-CMP-1 (a) and UPC-CMP-3 (b) sponge. The adsorption curves with different organic fractions in the presence of UPC-CMP-1 (c) and UPC-CMP-3 (d) coated sponges, benzene (PhH), toluene ($PhCH_3$) and chlorobenzene (PhCl).

on the framework of sponge to form superhydrophobic devices. The large-scale removal of organic solvents and removal of trace residual of organic contaminants can be realized in one device. To the best of our knowledge, the present work represents the first example that the stainless steel mesh or sponge were coated by superhydrophobic **CMP** material for rapid and efficient oil/water separation and water purification. The excellent separation efficiency and reusability together with its easy cleanness and storage make **UPC-CMP** coated device a perfect candidate for future practical application in oil/water separation and water purification, and the characteristics of easy coating on utensil surface enable this series of **CMP** materials to be used in more versatile devices.

Notes

The authors declare no competing financial interest.

Acknowledgements

This work was supported by the NSFC (Grant Nos. 21371179, 21571187), Taishan Scholar Foundation (ts201511019), and the Fundamental Research Funds for the Central Universities (13CX05010A, 14CX02150A, 15CX02069A, 15CX06074A).

Appendix A. Supplementary data

Supplementary data associated with this article can be found, in the online version, at http://dx.doi.org/10.1016/j.cej.2017.06.023.

References

[1] B. Wang, W. Liang, Z. Guo, W. Liu, Biomimetic super-lyophobic and super-lyophilic materials applied for oil/water separa-tion: a new strategy beyond nature, Chem. Soc. Rev. 44 (2015) 336–361.
[2] C. Gao, Z. Sun, K. Li, Y. Chen, Y. Cao, S. Zhang, L. Feng, Integrated oil separation and water purification by a double-layer TiO_2-based mesh, Energy Environ. Sci. 6 (2013) 1147–1151.
[3] J. Zhang, S. Seeger, Polyester materials with superwetting silicone nanofilaments for oil/water separation and selective oil absorption, Adv. Funct. Mater. 21 (2011) 4699–4704.
[4] X. Du, S. You, X. Wang, Q. Wang, J. Lu, Switchable and simultaneous oil/water separation induced by prewetting with a superamphiphilic self-cleaning mesh, Chem. Eng. J. 313 (2017) 398–403.
[5] X. Liu, Y. Wang, Z. Chen, K. Ben, Z. Guan, A self-modification approach toward transparent superhydrophobic glass for rainproofing and superhydrophobic fiberglass mesh for oil–water separation, Appl. Surf. Sci. 360 (2016) 789–797.
[6] L. Zhang, L. Li, Z. Dang, Bio-inspired durable, superhy-drophobic magnetic particles for oil/water separation, J. Colloid Interface Sci. 463 (2016) 266–271.
[7] C. Zhou, J. Cheng, K. Hou, A. Zhao, P. Pi, X. Wen, S. Xu, Superhydrophilic and underwater superoleophobic titania nanowires surface for oil repellency and oil/water separation, Chem. Eng. J. 301 (2016) 249–256.
[8] E. Cho, C. Chang-Jian, H. Chen, K. Chuang, J. Zheng, Y. Hsiao, K. Lee, J. Huang, Robust multifunctional superhydrophobic coatings with enhanced water/oil separation, self-cleaning, anti-corrosion, and anti-biological adhesion, Chem. Eng. J. 314 (2017) 347–357.
[9] A. Raza, B. Ding, G. Zainab, M. El-Newehy, S.S. Al-Deyab, J. Yu, In situ cross-linked superwetting nanofibrous membranes for ultrafast oil–water separation, J. Mater. Chem. A 2 (2014) 10137–10145.
[10] H. Sai, R. Fu, L. Xing, J. Xiang, Z. Li, F. Li, T. Zhang, Surface modification of bacterial cellulose aerogels' web-like skeleton for oil/water separation, ACS Appl. Mater. Interface 7 (2015) 7373–7381.
[11] C. Su, H. Yang, S. Song, B. Lu, R. Chen, A magnetic superhydrophilic/oleophobic sponge for continuous oil-water separation, Chem. Eng. J. 309 (2017) 366–373.
[12] Y. Li, X.J. Huang, S.H. Heo, C.C. Li, Y.K. Choi, W.P. Cai, S.O. Cho, Superhydrophobic bionic surfaces with hierarchical microsphere/SWCNT composite arrays, Langmuir 23 (2007) 2169–2174.
[13] Z. Chu, Y. Feng, S. Seeger, Oil/water separation with selective superantiwetting/superwetting surface materials, Angew. Chem. Int. Ed. 54 (2015) 2328–2338.
[14] C. Luo, X. Heng, Separation of oil from a water/oil mixed drop using two nonparallel plates, Langmuir 30 (2014) 10002–10010.
[15] L. Wu, J. Zhang, B. Li, A. Wang, Magnetically driven super durable superhydrophobic polyester materials for oil/water separation, Polym. Chemuk. 5 (2014) 2382–2390.
[16] Y. Hu, Y. Zhu, H. Wang, C. Wang, H. Li, X. Zhang, R. Yuan, Y. Zhao, Facile preparation of superhydrophobic metal foam for durable and high efficient continuous oil-water separation, Chem. Eng. J. 322 (2017) 157–166.
[17] L. Zhang, H. Li, X. Lai, X. Su, T. Liang, X. Zeng, Thiolated graphene-based superhydrophobic sponges for oil-water separation, Chem. Eng. J. 316 (2017) 736–743.
[18] Z. Xue, S. Wang, L. Lin, L. Chen, M. Liu, L. Feng, L. Jiang, L.A. Novel, Superhydrophilic and underwater superoleophobic hydrogel-coated mesh for oil/water separation, Adv. Mater. 23 (2011) 4270–4273.
[19] J. Yang, L. Yin, H. Tang, H. Song, X. Gao, K. Liang, C. Li, Polyelectrolyte-fluorosurfactant complex-based meshes with superhydrophilicity and superoleophobicity for oil/water separation, Chem. Eng. J. 268 (2015) 245–250.
[20] K. Jayaramulu, K.K.R. Datta, C. Rösler, M. Petr, M. Otyepka, R. Zboril, R.A. Fischer, Biomimetic superhydrophobic/superoleophilic highly fluorinated graphene oxide and ZIF-8 composites for oil-water separation, Angew. Chem. Int. Ed. 55 (2016) 1178–1182.
[21] X. Zhou, Z. Zhang, X. Xu, F. Guo, X. Zhu, X. Men, B. Ge, Robust and durable superhydrophobic cotton fabrics for oil/water separation, ACS Appl. Mater. Interface 5 (2013) 7208–7214.
[22] J. Jiang, F. Su, A. Trewin, C.D. Wood, H. Niu, J.T.A. Jones, Y.Z. Khimyak, A.I. Cooper, Synthetic control of the pore dimension and surface area in conjugated microporous polymer and copolymer networks, J. Am. Chem. Soc. 130 (2008) 7710–7720.
[23] U.H.F. Bunz, K. Seehafer, F.L. Geyer, M. Bender, I. Braun, E. Smarsly, J. Freudenberg, Porous polymers based on aryleneethynylene building blocks, Macromol. Rapid Commun. 35 (2014) 1466–1496.
[24] A. Thomas, Functional materials: from hard to soft porous frameworks, Angew. Chem. Int. Ed. 49 (2010) 8328–8344.
[25] D.D. Medina, J.M. Rotter, Y. Hu, M. Dogru, V. Werner, F. Auras, J.T. Markiewicz, P. Knochel, T. Bein, Room tem-perature synthesis of covalent-organic framework films through vapor-assisted conversion, J. Am. Chem. Soc. 137 (2015) 1016–1019.
[26] H. Yang, Y. Du, S. Wan, G.D. Trahan, Y. Jin, W. Zhang, Mesoporous 2D covalent organic frameworks based on shape-persistent arylene-ethynylene macrocycles, Chem. Sci. 6 (2015) 4049–4053.
[27] Y. Zeng, R. Zou, Z. Luo, H. Zhang, X. Yao, X. Ma, R. Zou, Y. Zhao, Covalent organic frameworks formed with two types of covalent bonds based on orthogonal reactions, J. Am. Chem. Soc. 137 (2015) 1020–1023.
[28] B. Teng, C. Pei, D. Zhang, J. Xu, F. Deng, X. Jing, S. Qiu, Gas storage in porous aromatic frameworks (Pafs), Energy Environ. Sci. 4 (2011) 3991–3999.
[29] D. Yuan, W. Lu, D. Zhao, H. Zhou, Highly Stable porous polymer networks with exceptionally high gas-uptake capacities, Adv. Mater. 23 (2011) 3723–3725.
[30] S. Wan, F. Gándara, A. Asano, H. Furukawa, A. Saeki, S.K. Dey, L. Liao, M.W. Ambrogio, Y.Y. Botros, X. Duan, S. Seki, J.F. Stoddart, O.M. Yaghi, Covalent organic frameworks with high charge carrier mobility, Chem. Mater. 23 (2011) 4094–4097.
[31] S. Lin, C.S. Diercks, Y.B. Zhang, N. Kornienko, E.M. Nichols, Y. Zhao, A.R. Paris, D. Kim, P. Yang, O.M. Yaghi, C.J. Chang, Covalent organic frameworks comprising cobalt porphyrins for catalytic CO_2 reduction in water, Science 349 (2015) 1208–1213.
[32] F.J. Uribe-Romo, C.J. Doonan, H. Furukawa, K. Oisaki, O.M. Yaghi, Crystalline covalent organic frameworks with hydrazone linkages, J. Am. Chem. Soc. 133 (2011) 11478–11481.
[33] F.J. Uribe-Romo, J.R. Hunt, H. Furukawa, C. Klöck, M.O. Keeffe, O.M. Yaghi, Crystalline imine-linked 3-D porous covalent organic framework, J. Am. Chem. Soc. 131 (2009) 4570–4571.
[34] X. Chen, M. Addicoat, E. Jin, L. Zhai, H. Xu, N. Huang, Z. Guo, L. Liu, S. Irle, D. Jiang, Locking covalent organic frameworks with hydrogen bonds: general and remarkable effects on crystalline structure, physical properties, and photochemical activity, J. Am. Chem. Soc. 137 (2015) 3241–3247.
[35] S. Jin, M. Supur, M. Addicoat, K. Furukawa, L. Chen, T. Nakamura, S. Fukuzumi, S. Irle, D. Jiang, Creation of superheterojunction polymers via direct polycondensation: segregated and bicontinuous donor-acceptor π-columnar arrays in covalent organic frameworks for long-lived charge separation, J. Am. Chem. Soc. 137 (2015) 7817.
[36] X. Liu, Y. Xu, Z. Guo, A. Nagai, D. Jiang, Super absorbent conjugated microporous polymers: a synergistic structural effect on the exceptional uptake of amines, Chem. Commun. 49 (2013) 3233–3235.
[37] X. Feng, L. Chen, Y. Dong, D. Jiang, Porphyrin-based two-dimensional covalent organic frameworks: synchronized synthetic control of macroscopic structures and pore parameters, Chem. Commun. 47 (2011) 1979–1981.
[38] A.H.S.A. An, S.L.A.W.B. Li, Superhydrophobic con-jugated microporous polymers for separation and adsorption, Energy Environ. Sci. 4 (2011) 2062–2065.
[39] Z. Xiao, Y. Zhou, X. Xin, Q. Zhang, L. Zhang, R. Wang, D. Sun, Iron(III) porphyrin-based porous material as photocatalyst for highly efficient and selective degradation of congo red, Macromol. Chem. Phys. 217 (2016) 599–604.
[40] Q. Lin, J. Lu, Z. Yang, X.C. Zeng, J. Zhang, Porphyrinic porous organic frameworks: preparation and post-synthetic modification via demetallation–remetallation, J. Mater. Chem. A 2 (2014) 14876–14882.
[41] S. Álvarez-Torrellas, J.A. Peres, V. Gil-Álvarez, G. Ovejero, J. García, Effective adsorption of non-biodegradable pharmaceuticals from hospital wastewater with different carbon materials, Chem. Eng. J. 320 (2017) 319–329.